


# Delineating hazardous CO<sub>2</sub> fluxes from acid mine drainage

Kwame Awuah-Offei<sup>1</sup> · Sisi Que<sup>2</sup>  · Moagabo Mathiba<sup>3</sup>

Received: 22 March 2015 / Accepted: 8 September 2015  
© Springer-Verlag Berlin Heidelberg 2015

**Abstract** Incidents of hazardous accumulations of CO<sub>2</sub> in homes built on or near reclaimed mine land, in the last decade, have been shown to be linked to neutralization reactions between acidic mine drainage and carbonate material. Recent research has shown that CO<sub>2</sub> fluxes on reclaimed mine land with this hazard are, sometimes, spatially autocorrelated (i.e., the spatial variability is not random). This result implies geostatistics can be used to delineate hazardous areas where fluxes are likely to exceed established thresholds. This study applies sequential Gaussian simulation to delineate this emerging hazard on a site in southwestern Indiana, USA. Due to lack of regulatory threshold limits for CO<sub>2</sub> flux at the current time, the authors conduct a sensitivity analysis of the threshold limit using the 75th, 90th and 95th percentiles of the measured fluxes for the first day of monitoring. These limits are used to produce hazard maps, which are validated with the known hazard at the site. This work further shows the potential of surface CO<sub>2</sub> flux monitoring as a cheap and effective strategy to monitor and delineate such hazards to

avoid residential and commercial real estate development in high risk zones.

**Keywords** CO<sub>2</sub> fluxes · Hazard delineation · Acid mine drainage · Mine reclamation · Sequential Gaussian simulation

## Introduction

In natural soils, the main source of soil CO<sub>2</sub> is plant root and microbial respiration, referred to just as soil respiration (Davidson et al. 1998; 2000; Pihlatie et al. 2007). Other sources, on local scales, include volcanoes, geothermal springs (Bergfeld et al. 2001; Chiodini et al. 2008; Lewicki et al. 2008), and dissolution of limestone by weakly, acidic precipitation. This work focuses on the recently identified source of hazardous soil CO<sub>2</sub>: neutralization reactions between acid mine drainage (AMD) and carbonate minerals in coal mine spoils and metal mines' wastes containing sulfide minerals (Ehler 2002; Lahmira et al. 2009). AMD-derived CO<sub>2</sub> may lead to potentially lethal concentrations of the gas accumulating in homes and structures constructed on, or adjacent to, reclaimed mine spoils.

Elevated levels of AMD-derived CO<sub>2</sub> are an emerging environmental, health and safety hazard associated with reclaimed mine land. CO<sub>2</sub> concentrations during episodes of CO<sub>2</sub> accumulation have exceeded recommended workplace safety thresholds (no thresholds exist for residential structures that the authors are aware of). There are documented cases of >25 % CO<sub>2</sub> concentration, which leads to low oxygen concentrations (<10 %) (Ehler 2002; Laughrey and Baldassare 2003; Robinson 2010). There is a need for economic and effective methods to identify the hazard (whether or not it exists) and delineate it (establish

---

✉ Sisi Que  
sq3g3@mst.edu

Kwame Awuah-Offei  
kwamea@mst.edu

Moagabo Mathiba  
mathibam@mopipi.ub.bw

<sup>1</sup> Missouri University of Science and Technology, 226 McNutt Hall, Rolla, MO 65409, USA

<sup>2</sup> School of River and Ocean Engineering, Chongqing Jiaotong University, Chongqing 400037, China

<sup>3</sup> Department of Civil Engineering, University of Botswana, Private Mail Bag 0061, Gaborone, Botswana

hazardous area boundaries), through field investigations and accurate mapping (Laughrey and Baldassare 2003; Robinson 2010).

Accumulation chamber trace gas monitoring has been used in various applications to delineate hazards from subsurface CO<sub>2</sub> (Farrar et al. 1995; Chiodini et al. 2008). To accomplish this, flux measurements are taken following valid protocols and the results used in geostatistical<sup>1</sup> analysis, which is used to infer the boundaries of the hazard, under uncertainty. A prerequisite of this kind of analysis is that the measured fluxes are spatially autocorrelated (i.e., the spatial variability is not random). This property has been well documented for CO<sub>2</sub> fluxes from volcanic and geothermal sources, whereas it has not been established for fluxes from soil respiration. For example, Lewicki et al. (2008) used sequential Gaussian simulation to investigate the relationship between meteorological variables, topography, and spatio-temporal variation of soil CO<sub>2</sub> fluxes at Mammoth Mountain, California, USA. Chiodini et al. (2008) used similar techniques to discriminate between hydrothermal and biogenic CO<sub>2</sub> at the Solfatara of Pozzuoli volcano degassing area in Naples, Italy. This work is of particular relevance because it shows how the use of properly defined thresholds can be used to delineate the area where each source is dominant.

However, such an approach has not yet been demonstrated feasible for AMD-CO<sub>2</sub> related hazards on reclaimed mine land. The relatively lower (compared to volcanic and geothermal) CO<sub>2</sub> fluxes, the heterogeneity of reclaimed mine soils, and differences in transport mechanisms make this hazard different from volcanic areas. However, without such an approach, the usefulness of accumulation chamber flux measurement for mitigation is limited, in this case. Recent research by the authors has shown that, in some instances, CO<sub>2</sub> fluxes on reclaimed mine land is spatially autocorrelated (Mathiba and Awuah-Offei 2015).

This result implies geostatistics can be used to predict the probability of the flux exceeding an established threshold at a location that has not been sampled using chamber flux measurement. The goal of this paper is to apply sequential Gaussian simulation to delineate the CO<sub>2</sub> hazard on a site in southwestern Indiana, USA, which has documented AMD-derived CO<sub>2</sub> and spatially autocorrelated fluxes (Mathiba and Awuah-Offei 2015). Due to the lack of established threshold limits (whether based on regulations or detailed isotope analysis—Chiodini et al. 2008) for CO<sub>2</sub> flux at this time, the authors conduct a sensitivity analysis of the threshold limit using the 75th,

90th and 95th percentiles of the measured fluxes. Three separate days of CO<sub>2</sub> flux data from the authors' previous research are used in this work (Mathiba et al. 2015; Mathiba and Awuah-Offei 2015). The spatial continuity of the fluxes is modeled using semi-variograms (assumption of second-order stationarity—Schabenberger and Gotway 2005), after data transformation. Sequential Gaussian simulation is used to estimate the probability of fluxes exceeding the thresholds, at each grid node, using the GS+ software (Gamma Design Software, LLC, Plainwell, MI, USA, [www.gammadesign.com](http://www.gammadesign.com)). The result is a set of probability of exceedance maps (or just exceedance maps), which are risk maps for delineating the hazard. This is to illustrate how risk maps can be produced, if thresholds are established for this hazard.

## Methods

### Study site

Field sampling was conducted at a reclaimed mine site in Indiana, United States of America (USA). This site has been the subject of CO<sub>2</sub> investigations to mitigate hazards in homes built on reclaimed mine spoil (Robinson 2010). The study site is located in Pike County, in southwestern Indiana (Latitude: 38° 19' 42" N and Longitude: 87° 08' 27" W). Robinson (2010) describes the site history. The soils are described as Fairpoint loam, reclaimed (unit FaB) at 1 to 15° slopes (Natural Resources Conservation Service (NRCS) 2009). The site is a reclaimed surface coal mine covering an area of about 36 hectares—the research team had access to only 18.5 hectares, which was studied in this work. Mining was carried out from 1986 to 1992 and the site was reclaimed with lime amendment and about 0.91 meters (3 ft) of top soil capping. The spoil material extends down for about 11.6 meters (40 ft) below the surface and the single story home, with a basement built on it. The home has been experiencing intermittent episodes of elevated concentrations of stray CO<sub>2</sub> in its basement since 2006 (Robinson 2010).

### CO<sub>2</sub> flux measurements

Soil CO<sub>2</sub> fluxes were measured at regular sampling grids at this site using accumulation chamber (AC) trace gas measurements (Parkin et al. 2003). Soil CO<sub>2</sub> fluxes were measured using an LI-8100-103 automated soil CO<sub>2</sub> flux monitoring system (Licor Biosciences, Inc., Lincoln, Nebraska). Collars (100 mm high) were made from 200 mm diameter PVC pipes. Collars were inserted into the soil to leave 20 mm of collar above the soil (Parkin et al. 2003). All collars were installed at least 24 h prior to

<sup>1</sup> Geostatistics is used in this work to mean the field of spatial statistics that deals with continuous domains (Schabenberger and Gotway 2005, p. 6). The authors are aware that some authors do not consider simulation of random fields a “geostatistical” technique. We choose this broader definition for convenience.

flux measurements to allow the soil gas fluxes to stabilize after initial disturbance from installation. The chamber was deployed for a short period, 2 min, to minimize pressure buildup, which may impact the CO<sub>2</sub> flux and lead to flux underestimation. Sampling was conducted on March 30 and 31, and April 2, 2010. It involved 138 sampling points (Fig. 1) on a 22.9 m × 45.7 m (75 ft × 150 ft) grid except for the north-eastern boundary, where samples were 45.7 m (150 ft) apart. A few additional sampling points were placed around the house, constructed on the site.

**Delineating AMD-derived CO<sub>2</sub> hazard**

Geostatistics can be used for hazard delineation if the hazard indicator variable is spatially correlated (Farrar et al. 1995, 1998; Chiodini et al. 2008). An initial step in geostatistics is to describe the spatial correlation of the random field. This is done using correlation functions or semi-variograms, which assume the random field is second-order stationary (Schabenberger and Gotway 2005). In this work, semi-variograms are used to describe the spatial correlation structure of CO<sub>2</sub> fluxes from the study site. Input from the semi-variogram analysis is then used to predict CO<sub>2</sub> fluxes at nodes of a regular grid using sequential Gaussian simulation (sGs). This is then used to produce exceedance maps at various thresholds.

**Preliminary data analysis and transformation**

Figure 2 shows the fluxes measured on all three days. It shows significant spatial variability with the range (difference between minimum and maximum) of fluxes

between 9.19 and 10.65 μmol m<sup>-2</sup> s<sup>-1</sup>. Table 1 shows summary statistics of soil CO<sub>2</sub> flux data from the study site. The fluxes were found to be positively skewed according to the Anderson–Darling normality test (*p* < 0.005) for all sampling days (Table 1), indicating that the datasets were non-normal. These datasets were log-transformed in an attempt to make them normally distributed since ensuing analysis assume normality. After log-transforming the data, the non-normality was removed as indicated by the lower A<sup>2</sup> values with higher *p* values (*p* > 0.05) (Table 1). Probability plots of the data visually confirm this (Fig. 3). The probability plots of the raw data show distinct non-linearity while the log-transformed flux data plot on a fairly straight line as expected for lognormally distributed data.

As indicated in the “Introduction”, a prerequisite of spatial statistical analysis is that the data is spatially autocorrelated. The full discussion of observed spatial autocorrelation in this dataset has been presented elsewhere (Mathiba and Awuah-Offei 2015). Summary results are repeated here for the reader’s benefit. Table 2 shows the results of tests for spatial autocorrelation using the Moran’s I statistic (Schabenberger and Gotway 2005). The results show that the data sets are all significantly spatially autocorrelated at 95 % confidence (*p* < 0.05). Spatial autocorrelation is important for geostatistical modeling, which is the goal of this work. Prior to the work by Mathiba and Awuah-Offei (2015), spatial variation in CO<sub>2</sub> fluxes on reclaimed mine land had been attributed to high variability in soil properties in reclaimed mine soil. Our work shows that, under certain conditions, spatial autocorrelation exist in CO<sub>2</sub> fluxes on reclaimed mine land since the generation phenomenon is not controlled solely by the soil biological activity. Table 2 shows the study site is a good case study for such application of spatial statistical techniques. This shows that the premise of the research (i.e., geostatistical delineation of hazards) is viable under the conditions at the study site.

**Semi-variogram modeling**

The experimental semi-variogram (also referred to as sample or empirical semi-variogram) is an approximation of a theoretical semi-variance ( $\frac{1}{2}E[(Z(\mathbf{x}) - Z(\mathbf{x} + \mathbf{h}))^2]$ ) for describing the mean squared variance of an attribute, in this case CO<sub>2</sub> flux, over a lag distance **h** apart and can be defined by Eq. (1):

$$\gamma(\mathbf{h}) = \frac{1}{2N(\mathbf{h})} \sum_{\forall N(\mathbf{h})} (Z(\mathbf{x}) - Z(\mathbf{x} + \mathbf{h}))^2 \tag{1}$$

where  $\gamma(\mathbf{h})$  is the semi-variance; **h** is the lag distance;  $z(\mathbf{x} + \mathbf{h})$  and  $z(\mathbf{x})$  are the observed values of the CO<sub>2</sub> flux at sample points  $\mathbf{x} + \mathbf{h}$  and  $\mathbf{x}$ , respectively; and  $N(\mathbf{h})$  is the

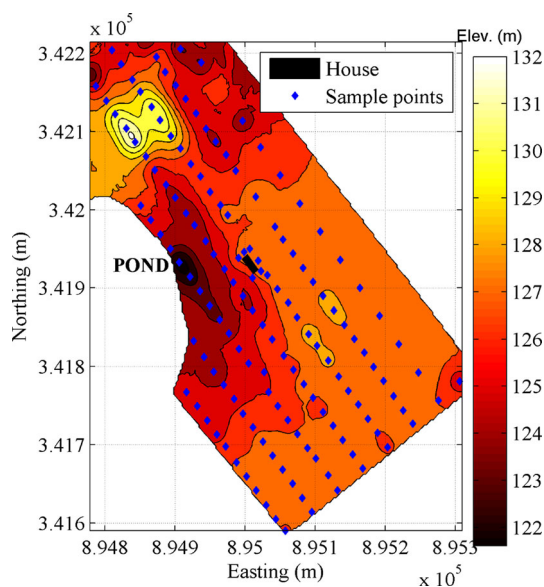


**Fig. 1** Pike County study site with sample points

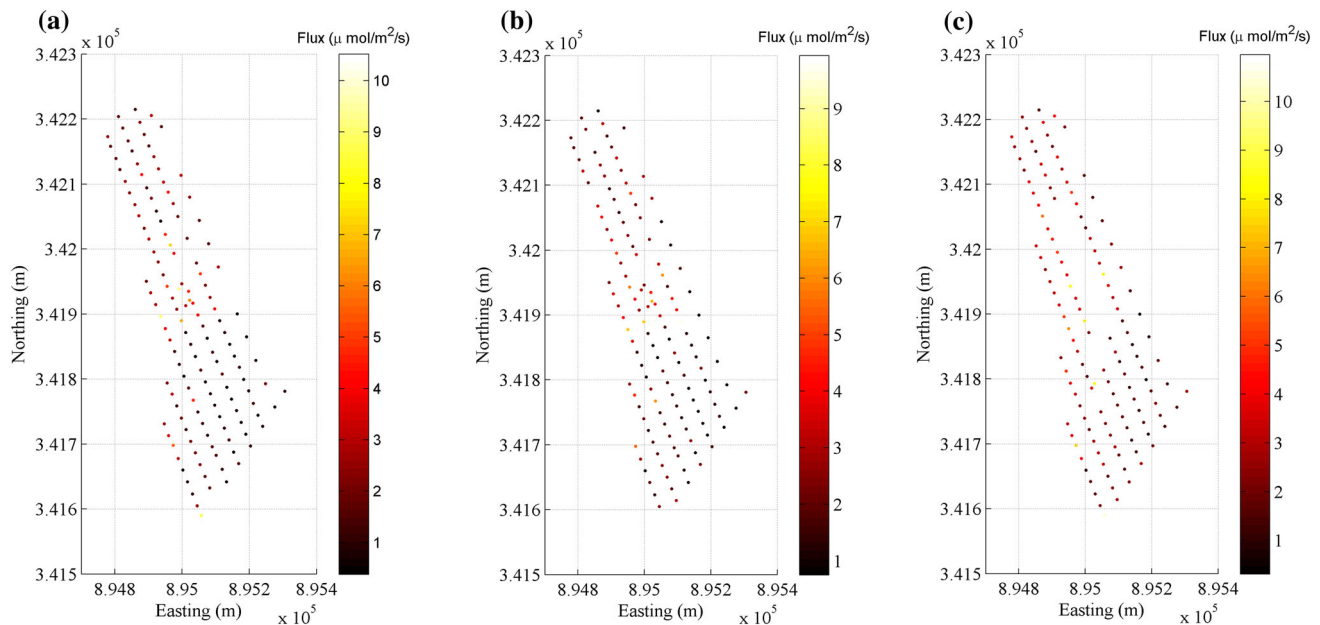


**Fig. 2** CO<sub>2</sub> fluxes **a** Day 1; **b** Day 2; and **c** Day 3

**Table 1** Summary statistics of raw CO<sub>2</sub> fluxes ( $\mu\text{mol m}^{-2} \text{s}^{-1}$ )

Sampling day	Day 1 (3/30/10)	Day 2 (3/31/10)	Day 3 (4/2/10)
Mean	2.35	2.58	2.96
Standard deviation	1.81	1.71	1.80
Variance	3.29	2.93	3.24
Coefficient of variation (%)	77	66.3	60.8
Skewness	2.17	2.17	2.11
Kurtosis	5.76	5.90	5.61
No. of samples	132	136	131
Minimum	0.38	0.75	0.31
1st quartile	1.11	1.47	1.79
Median	1.82	2.12	2.59
3rd quartile	2.87	3.11	3.59
Maximum	10.57	9.94	10.96
$F_{\text{CO}_2}$			
$A^2$	7.162	7.259	6.511
$p$ value	<0.005	<0.005	<0.005
$\log(F_{\text{CO}_2})$			
$A^2$	0.467	0.503	0.493
$p$ value	0.248	0.201	0.213

number of pairs  $h$  distance apart. Variogram modeling is necessary because the models we use in analysis should be conditionally negative definite (Schabenberger and Gotway 2005). Modeling also allows us to impose our understanding of the random field, gained from examining the

data, on the models of the spatial correlation. Modeling considers questions such as: (1) Is the random field isotropic or anisotropic? (2) Which theoretical model best represents the observed spatial correlation? (3) What are the optimal parameters of the model that best represents the observed spatial correlation? Three theoretical models were considered in the variogram modeling in this work: exponential, gaussian and spherical semi-variogram models. In modeling the spatial correlation, the random field was assumed to be isotropic. This assumption was necessary because there were not enough data to model directional semi-variograms. The authors' attempts to do this resulted in ill-behaved experimental semi-variograms in many directions because of low number of pairs. The results of modeling are shown in Fig. 4 and Table 3.

In some instances, ill-behaved semi-variograms in a particular direction are due to certain characteristics of the data that should be considered in the simulation processes. We did not conduct such an investigation in this work because of the limited data. However, we believe the effect of this on our overall conclusions is negligible because this work seeks to establish that these hazards can be delineated rather than put forth a concrete delineation of the hazard at the study site. Further data collection is required to explore anisotropy in the random field at the study site. This will establish whether the assumption of an isotropic CO<sub>2</sub> flux random field is valid or not. It could also define the nature of the anisotropy at the study site. Such work, although relevant, is beyond the scope of this work. We deem the assumption of an isotropic random field, which is

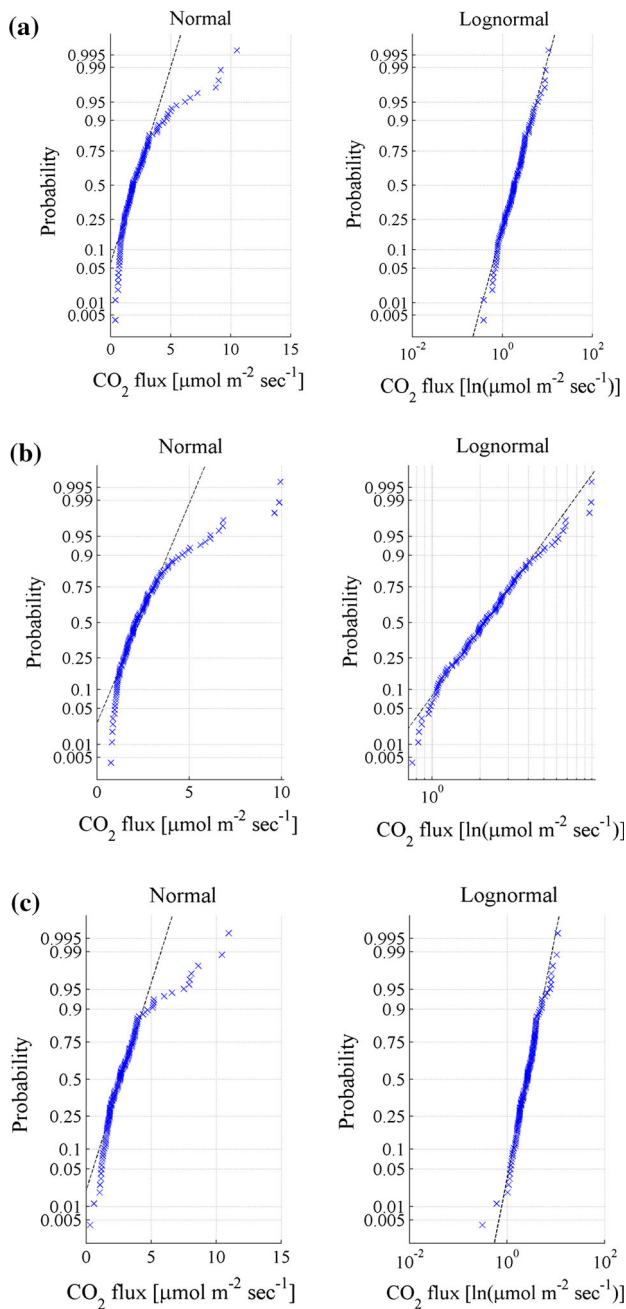


**Fig. 3** Raw and log-transformed distributions of flux for **a** day 1; **b** day 2; **c** day 3

**Table 2** Results of spatial autocorrelation hypothesis testing for CO<sub>2</sub> fluxed

Data set	No. of samples	Observed Moran's I	Expected value	p value
Day 1 (3/30/10)	131	0.481	-0.00763	<0.0001
Day 2 (3/31/10)	136	0.310	-0.00741	<0.0001
Day 3 (4/02/10)	131	0.292	-0.00763	<0.0001

common in many CO<sub>2</sub> flux analysis (Chiodini et al. 2008; Lewicki et al. 2008), to be adequate to illustrate how to delineate the hazard.

**Sequential Gaussian simulation**

Simulation is a geostatistical interpolation technique, which can be used for assessing uncertainty in the spatial distribution of an attribute, in this case CO<sub>2</sub> fluxes on reclaimed mine land. This is achieved by repeatedly generating equally likely realizations of the fluxes. Each simulated value in a realization is conditioned on the original data and previously simulated values. These realizations are then used to characterize a surface of the spatial distribution of the fluxes (Sun et al. 2008). Simulation offers the following advantages over traditional kriging: (1) it does not minimize the local error variance and, therefore, no smoothing effect; (2) simulation reproduces the spatial variability modeled from sample information, thus honoring the sample data; and (3) it produces a more realistic map, that is a realization of the random variable being simulated (Lin 2008; Sun et al. 2008).

In this work, the entire 18.5 hectares area of the study site was divided into 3 m × 3 m grids resulting in 20,354 grid nodes for prediction. A thousand realizations of CO<sub>2</sub> fluxes are simulated for each grid node, for each day, to produce maps of expected CO<sub>2</sub> fluxes (using a point-by-point average) and probability of exceedance maps of CO<sub>2</sub> fluxes in GS+ software (Gamma Design Software, LLC, Plainwell, MI, USA, [www.gammadesign.com](http://www.gammadesign.com)). In the simulation, the search neighborhood was circular (isotropic) and the authors used the semi-variogram range as the search radii. In addition, the number of points used in estimation was limited to between 3 and 16.

At the current time, no regulatory threshold limits exist for CO<sub>2</sub> fluxes to regulate hazards. Up until now, researchers have conducted only limited isotopic characterization at the study site. Since this precluded the authors from developing rigorous thresholds based on evidence (data), arbitrary limits are set at 75th, 90th and 95th percentiles of the measured values to produce hazard risk maps. This is to illustrate how risk maps can be produced,

**Fig. 4** Semi-variogram modeling of log of CO<sub>2</sub> flux: **a** Day 1; **b** Day 2; **c** Day 3

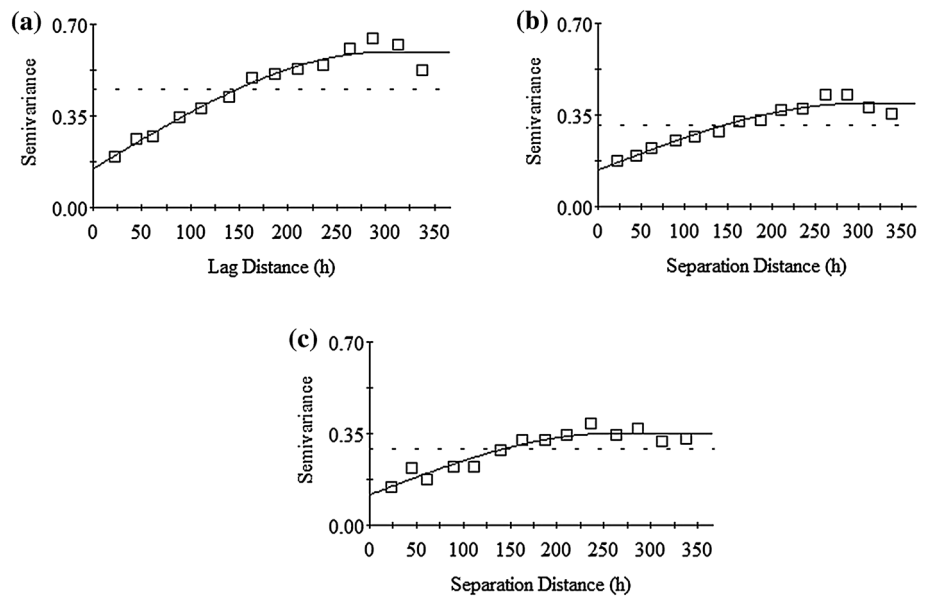


**Table 3** Semi-variogram models

Day	Model	Nugget [ $\log(\mu\text{mol m}^{-2} \text{s}^{-1})]^2$	Sill [ $\log(\mu\text{mol m}^{-2} \text{s}^{-1})]^2$	Range (m)	$R^2$
1	Spherical	0.148	0.594	298.7	0.959
2	Spherical	0.140	0.394	299.5	0.941
3	Spherical	0.116	0.351	257.2	0.905

if thresholds are established and also to examine the sensitivity of the risk delineation to the threshold. To facilitate easy comparison of the resulting maps for all three days, the authors chose to use the 75th, 90th and 95th percentiles of the Day 1 data for all 3 days. These thresholds were 2.87, 4.59, and  $6.32 \mu\text{mol m}^{-2} \text{s}^{-1}$ , respectively.

## Results and discussions

Figure 5 shows flux simulation results for all 3 days. The authors checked the GS+ weighted back-transformation algorithm using the fluxes at the measured data points. Table 4 shows the results, which are deemed adequately consistent for this purpose. Figure 5 (and also Figs. 6, 7, 8) shows the outline of the house surrounded by the lawn area (white) and the barn adjacent (cyan) to the lawn. High fluxes appear to coincide with the lawn, with the very high fluxes around the house and to the southwest, towards the pond. Similar trends can be observed for all 3 days. It is reasonable to assume that periodic mowing returns more organic content into the soil, resulting in higher soil CO<sub>2</sub> production. However, even in the lawn, there are higher fluxes around the house and toward the pond. These could be the result of greater soil permeability for the post-construction soils (Jacinthe and Lal 2006), and abrupt changes

in topography. Jacinthe and Lal (2006) show that reduced soil macro-porosity from over compaction during reclamation can hamper soil-atmosphere CO<sub>2</sub> exchange. If this is, in fact, a key factor then it may explain the reduced fluxes everywhere else, but around the house where the soil has been disturbed by construction.

From the simulation results, total CO<sub>2</sub> emissions for the 18.5 hectares are estimated at 1.508, 1.514, and 1.844 t/day of CO<sub>2</sub> for March 30 and 31, and April 2, respectively. The average daily diffusion rate is 1.622 t/day. April 2 emissions were the highest, which is consistent with the observed fluxes (Table 1). These discharges are far lower than some of the hazardous volcanic-related CO<sub>2</sub> discharges reported in the literature. For example, the Horseshoe Lake tree kill area on Mammoth Mountain, California, which has been studied by various researchers, is only about three times larger than our study site (the Horseshoe Lake tree kill area is 50 hectares—Gerlach et al. 1998). Yet, Gerlach et al. (1998) estimated the average CO<sub>2</sub> diffusion rates to be approximately 250 t/day, which is 150 times more than the rates at our study site. Even in its decline, Lewicki et al. (2008) estimated the average daily discharge from the Horseshoe Lake tree kill area to be 38 t/day, which is still 23 times our estimate. It is understandable then why the CO<sub>2</sub> diffusion from reclaimed mine land does not lead to habitat degradation like these other

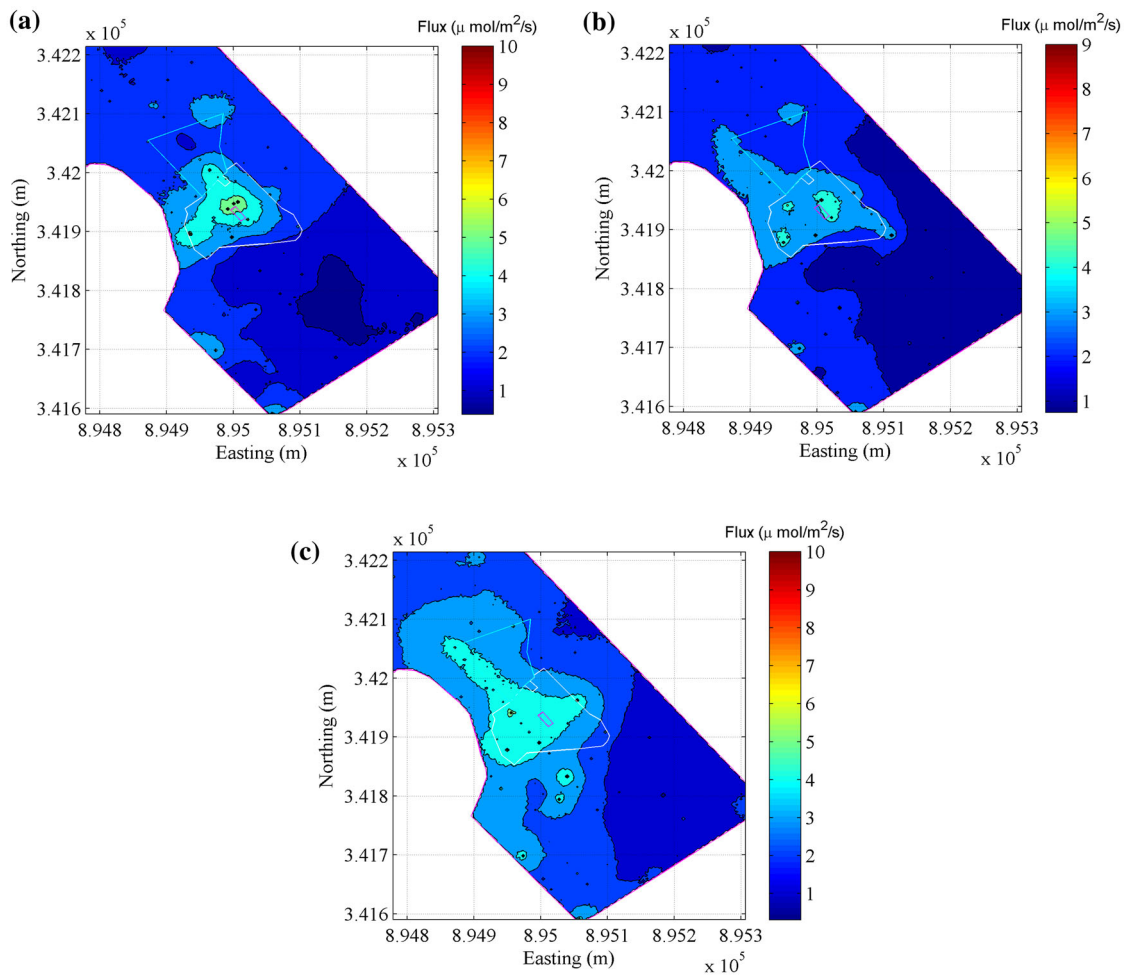


**Fig. 5** Simulation results showing average values of 1000 simulations for **a** Day 1; **b** Day 2; **c** Day 3

**Table 4** Verifying GS+ back-transformation results

Day	Original mean ( $\mu\text{mol m}^{-2} \text{s}^{-1}$ )	Back-transformed mean ( $\mu\text{mol m}^{-2} \text{s}^{-1}$ )	Original variance [ $(\mu\text{mol m}^{-2} \text{s}^{-1})^2$ ]	Back-transformed variance [ $(\mu\text{mol m}^{-2} \text{s}^{-1})^2$ ]
1	2.35	2.33	3.29	3.13
2	2.58	2.56	2.93	2.36
3	2.96	2.96	3.24	2.97

hazards. However, the danger of this hazard arises from accumulation of CO<sub>2</sub> in structures built on such land. So, whereas the low diffusion rates do not pose an obvious hazard, care should be taken to avoid high hazard areas and site development should be done in a way to mitigate the hazards. Carefully identifying and delineating the hazard is a starting point to achieve this goal.

Figures 6, 7, 8 show CO<sub>2</sub> hazard probability maps of all 3 days, which can be used for delineating high risk areas. The thresholds used for the probability plots are 2.87, 4.59,

and  $6.32 \mu\text{mol m}^{-2} \text{s}^{-1}$ , which are the 75th, 90th, and 95th percentiles, respectively, of the Day 1 data (to facilitate easy comparison). The general profile of the risk maps follows the spatial distribution of fluxes (Fig. 5).

When the results for all 3 days are compared, it is obvious that there is temporal variation in the high risk regions (defined here as >75 % probability of exceeding the threshold value). This is most obvious when Figs. 6a, 7a and 8a are compared to each other. The area of the high risk zone is highest for Day 3 and lowest for Day 2. For the same day, the high risk region decreases as the threshold value increases, as one would expect. For instance, for the Day 2 results, whereas there are pockets of high risk regions that have 75 % or more probability of exceeding  $2.87 \mu\text{mol m}^{-2} \text{s}^{-1}$ , there is no region with more than 20 % chance of exceeding  $6.32 \mu\text{mol m}^{-2} \text{s}^{-1}$  (Fig. 7). This shows that the exact value of the threshold value is very important, if this technique is to be used to enhance public safety.

The goal of this paper is to illustrate how to delineate high (above established threshold) CO<sub>2</sub> flux fields for post-

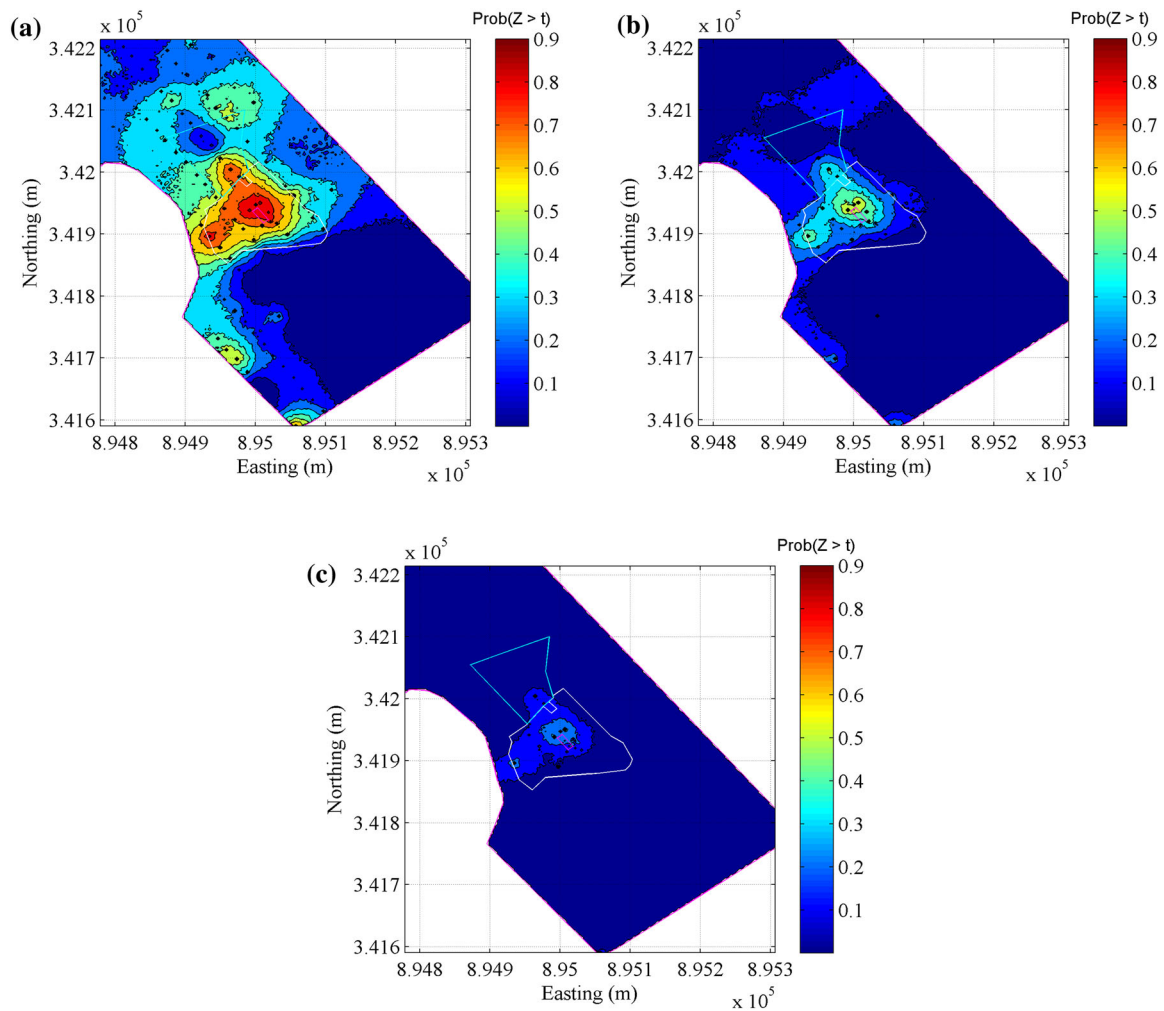


**Fig. 6** Threshold exceedance maps for Day 1. Probability of exceeding: **a** 2.87; **b** 4.59; **c** 6.32  $\mu\text{mol m}^{-2} \text{s}^{-1}$

mining land use decision making. Figures 6, 7, 8 show that this is possible with accumulation chamber flux monitoring. The remaining challenge is establishing thresholds, above which there is a high likelihood of  $\text{CO}_2$  accumulation in structures built on the land. The authors' research till date has failed to establish such thresholds for two reasons.

First, stable carbon isotope characterization using gas samples taken during flux monitoring has failed to clearly discriminate between regions with significant contribution from AMD-related  $\text{CO}_2$  to the flux and those without, based on isotopic composition of the  $\text{CO}_2$ . This is most likely due to the episodic nature of this hazard and the unique transport mechanisms (Mathiba et al. 2015, Mathiba 2013). It is possible the soil gas permeability is low under diffusive flux and, therefore, does not allow significant contribution of the deep AMD-related  $\text{CO}_2$  to the soil-atmospheric exchange under normal conditions. The residents of the house did not report any episode (the United States Geological Survey (Robinson 2010) had

installed  $\text{CO}_2$  monitors in the basement to trigger an alarm, if there was an episode) during the monitoring period. Low contribution from AMD-related  $\text{CO}_2$  will not change the isotopic signature significantly (to the point where there is a distinct difference between the observed stable carbon isotope ratios and known/expected biogenic  $\text{CO}_2$ ). It is also possible that the native  $\text{CO}_2$  gasses already have significantly lower  $^{13}\text{C}:^{12}\text{C}$  ratio, so that the changes due to the limestone source are not obvious.

Second, no multi-modal distributions of  $\text{CO}_2$  fluxes have been observed till date (Mathiba et al. 2015). Such multi-modal distributions could provide a basis for establishing a threshold, especially when confirmed with isotope ratio mass spectroscopy (Chiodini et al. 2008). Possibly because of the low contribution under normal conditions, no bimodal distributions were observed in the data (Fig. 3). Such bimodal distributions represent as a curve with a point of inflection in it, on a probability plot (Chiodini et al. 2008). The observed distributions were skewed, like most geoscience data and shown to be lognormally distributed.



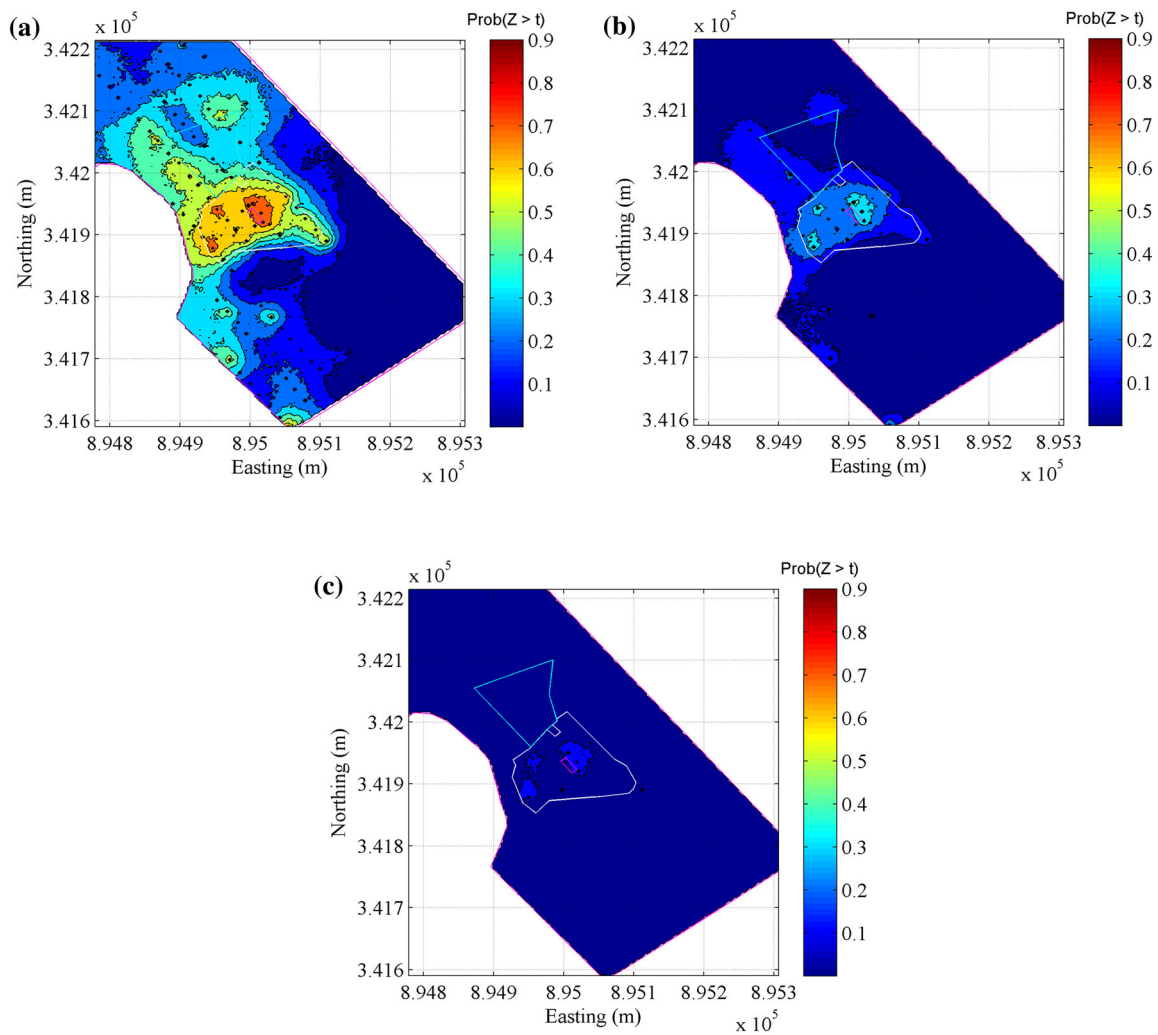


**Fig. 7** Threshold exceedance maps for Day 2. Probability of exceeding: **a** 2.87; **b** 4.59; **c** 6.32  $\mu\text{mol m}^{-2} \text{s}^{-1}$

The authors hypothesize that the situation changes when sudden drops in barometric pressure induce advective fluxes, which result in significant flow of the deep AMD-related CO<sub>2</sub>. Testing this hypothesis is beyond the scope of this paper and should be part of future work to identify hazard threshold limit fluxes.

These two reasons do not necessarily mean such a threshold does not exist or cannot be established with further research. Further research is required to establish reliable hazard thresholds that are shown to be correlated to the likelihood of dangerous CO<sub>2</sub> accumulation in homes built on the reclaimed land. The challenge is compounded by the temporal variation as well. Hence, future accumulation chamber monitoring should be done through continuous long-term monitoring using a monitor suited for the purpose. Such a monitor can sample several strategically located sample points at specified time intervals over a year or more. Ideally, the monitoring should be on reclaimed mine land with the hazard and control properties so that

differences in spatio-temporal variability of fluxes can be observed to inform threshold conclusions. Otherwise, establishing high thresholds that occur only when there is an episode could lead to regulators declaring land useful for real estate development (because “high” fluxes were not observed) only to find out fluxes do reach such levels after construction and/or during episodes. Such work is vital in areas like eastern United States where pressure on land use is causing increasing use of reclaimed mine land for real estate.

### Conclusion

This study applies sequential Gaussian simulation to delineate hazardous zones on a reclaimed mine site in southwestern Indiana, USA, with documented CO<sub>2</sub> hazard related to reactions between acid mine drainage (AMD) and carbonate minerals. Due to lack of regulatory threshold

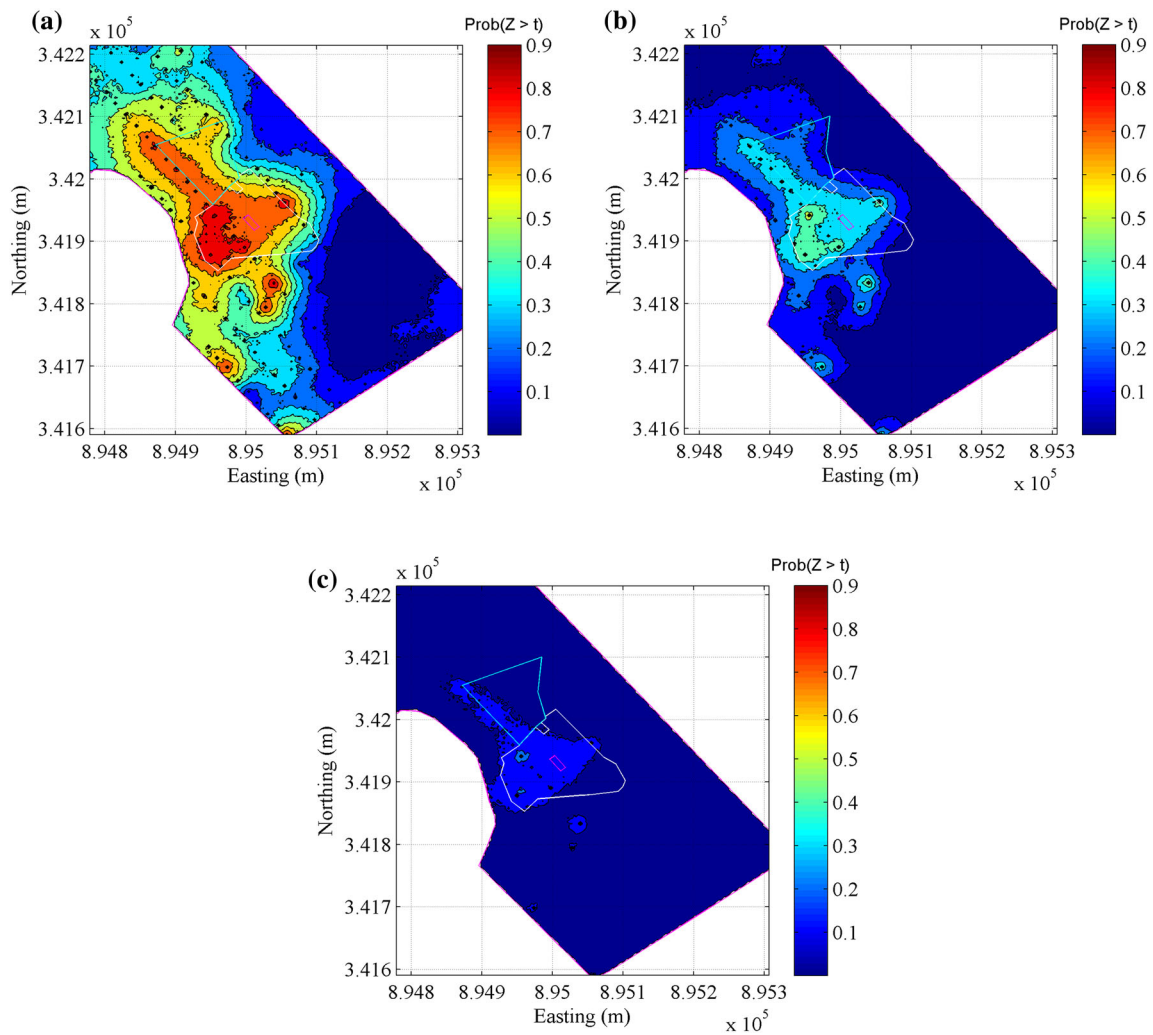


**Fig. 8** Threshold exceedance maps for Day 3. Probability of exceeding: **a** 2.87; **b** 4.59; **c** 6.32  $\mu\text{mol m}^{-2} \text{s}^{-1}$

limits for  $\text{CO}_2$  flux at the current time, the authors conduct a sensitivity analysis of the threshold limit using the 75th, 90th and 95th percentiles of the measured fluxes on the first day of monitoring. These limits are used to produce hazard maps, which are validated with the known hazard at the site (accumulation in the house built on the land). The results show that hazard maps can be produced that clearly correlate to risk levels and can be useful for post-mining land use planning. The results also show that total diffusion rates from the study site are far below the rates of volcanic  $\text{CO}_2$  hazards, which can cause habitat damage. However, the danger of significant accumulation in homes built on such land warrants research to delineate such hazards. This work further demonstrates the potential of surface  $\text{CO}_2$  flux monitoring as a cheap and effective strategy to monitor and delineate such hazards to avoid residential and commercial real estate development on high risk zones. Future work should attempt to establish hazard thresholds for this hazard.

**Acknowledgments** The authors would like to acknowledge: Office of Surface Mining, Reclamation and Enforcement's Applied Science program's project #S09AC15437 and the Government of Botswana for financial support; Dr. Bret A. Robinson for his assistance in accessing the study site; Alfred J. Baldassare for his input; and Bismark Osei for his assistance in this work.

The authors are also grateful for the review comments in response to our original submission. The comments have improved the quality of the manuscript.

## References

- Bergfeld D, Goff F, Janik CJ (2001) Elevated carbon dioxide flux at the dixie valley geothermal field, Nevada: relations between surface phenomena and the geothermal reservoir. *Chem Geol* 117:43–66
- Chiodini G, Caliro S, Cardellini C, Avino R, Granieri D, Schmidt A (2008) Carbon isotopic composition of soil  $\text{CO}_2$  efflux, a powerful method to discriminate different sources feeding soil  $\text{CO}_2$  degassing in volcanic-hydrothermal areas. *Earth Planetary Sci Lett* 274:372–379

- Davidson EA, Belk E, Boone R (1998) Soil water content and temperature as independent or confounded factors controlling soil respiration in a temperate mixed hardwood forest. *Glob Chang Biol* 4:217–227
- Davidson EA, Verchot LV, Cattânio JH, Ackerman IL, Carvalho JEM (2000) Effects of soil water content on soil respiration in forests and cattle pastures of Eastern Amazonia. *Biogeochemistry* 48:53–69
- Ehler WC (2002) Dangerous atmosphere created by strip mine spoil. *The Proceedings of the 24th National Association of Abandoned Mine Lands Programs*. Park City, Utah, pp 1–16
- Farrar CD et al. (1998) Magmatic Carbon Dioxide Emissions at Mammoth Mountain, California. US Geological Survey. *Water-Resources Investigations Report*, pp 98–4217
- Farrar CD et al (1995) Forest-killing diffuse CO<sub>2</sub> emission at Mammoth Mountain as a sign of magmatic unrest. *Nature* 376:675–678
- Gerlach TM, Doukas MP, McGee KA, Kessler R (1998) Three-year decline of magmatic CO<sub>2</sub> emissions from soils of a Mammoth Mountain tree kill: Horseshoe Lake, CA, 1995–1997. *Geophys Res Lett* 25:1947–1950
- Jacinte PA, Lal R (2006) Spatial variability of soil properties and trace gas fluxes in reclaimed mine land in Southeastern Ohio. *Geoderma* 136:598–608
- Lahmira B, Lefebvre R, Hockley D, Phillip M (2009). Sullivan Mine fatalities incident: Numerical modeling of gas transport and reversal in gas flow directions. Presented in the securing the future and 8th International Conference on Acid Rock Drainage (ICARD), June 2–26, 2009, Skelleftea, Sweden
- Laughrey Christopher D, Baldassare Fred J (2003) Some applications of isotope geochemistry for determining sources of stray carbon dioxide gas. *Environ Geosci* 10(3):107–122
- Lewicki JL, Fischer ML, Hilley GE (2008) Six-week time series of Eddy Covariance CO<sub>2</sub> Flux at Mammoth Mountain, California: performance evaluation and role of meteorological forcing. *J Volcanol Geoth Res* 171:178–190
- Lin YP (2008) Simulating Spatial distributions, variability and uncertainty of soil arsenic by geostatistical simulations in geographical information systems. *The Open Environ J* 2:26–33
- Mathiba M (2013) Spatial variation of AMD related CO<sub>2</sub> emissions on reclaimed mine spoil. Dissertation. Missouri University of Science and Technology
- Mathiba M, Awuah-Offei K (2015) Spatial autocorrelation of soil CO<sub>2</sub> fluxes on reclaimed mine land. *Environ Earth Sci* 73(12):8287–8297
- Mathiba M, Awuah-Offei K, Baldassare FJ (2015) Influence of elevation, soil temperature and soil moisture content on reclaimed mine land soil CO<sub>2</sub> fluxes. *Environ Earth Sci* 73(10):6131–6143
- Natural Resources Conservation Service (NRCS). (2009) Web Soil Survey. Retrieved June 6, 2011, from USDA NRCS Website: <http://websoilsurvey.nrcs.usda.gov/app/WebSoilSurvey.aspx>
- Parkin T, Mosier A, Smith J, Venterea R, Johnson J, Reicosky D et al. (2003) Chamber-based trace gas flux measurement protocol. USDA-ARS
- Pihlatie M, Pumpanen J, Rinne J, Ilvesniemi H, Simojoki A, Hari P, Vesela T (2007) Gas concentration driven fluxes of nitrous oxide and carbon dioxide in boreal forest soil. *Tellus* 59B(3):458–469
- Robinson BA (2010) Occurrence and attempted mitigation of carbon dioxide in a home constructed on reclaimed coal-mine spoil, Pike County, Indiana. US Geological Survey Scientific Investigations Report 2010-5157, p 21
- Schabenberger O, Gotway CA (2005) Statistical methods for spatial data analysis. Chapman and Hall/CRC, Boca Raton
- Sun Y, Ding N, Cai F, Meng F (2008) Spatial analysis of heavy metals in surface soils based on geostatistics. In: *Proceedings of SPIE*, vol 7145, pp 714514